Load Pushing Capacity Analysis of Individual and Multi-Cooperative Mobile Robot through Symbiotic Application

Arvin H. Fernando [1,*], Marielet A. Guillermo [2], Laurence A. Gan Lim [1], Argel A. Bandala [3], Ryan Rhay P. Vicerra [2], Elmer P. Dadios [2], and Raouf N. G. Naguib [4]

[1] Department of Mechanical Engineering, De La Salle University, Manila, Philippines
[2] Department of Manufacturing Engineering and Management, De La Salle University, Manila, Philippines
[3] Department of Electronics and Computer Engineering, De La Salle University, Manila, Philippines
[4] Department of Mathematics, Computer Science and Engineering, Liverpool Hope University, Liverpool, UK
Email: arvin.fernando@dlsu.edu.ph (A.H.F.); marielet.guillermo@dlsu.edu.ph (M.A.G.); laurence.ganlim@dlsu.edu.ph (L.A.G.L.); argel.bandala@dlsu.edu.ph (A.A.B.), ryan.vicerra@dlsu.edu.ph (R.R.P.V.); elmer.dadios@dlsu.edu.ph (E.P.D.); r.naguib@ieee.org (R.N.G.N.)
*Corresponding author

***Abstract*—Certain missions require multiple mobile robots working together to accomplish it. There is a need, however, to determine the optimal configuration of modular mobile robots doing cooperative tasks to ensure high utilization and efficiency rate of the individual robot. This study proposed the use of a biosystem-inspired approach in assessing the influence of multiple robots on each other in performing a cooperative pushing task. The kinematics of pushing interaction at a single contact point was first discussed in the study to provide a solid foundation of the mission to be analyzed. Various dimensions in an experimental setup were also covered to better understand how these contribute to planar pushing. Through the resulting symbiotic coefficient, the study was able to determine the optimal configuration among the two, four, and six wheeled mobile robots pushing an object with various loads. While the dominant coefficient for symbiotic relationship was classified as beneficial and only one was neutral, the decline in coefficient values of the 3rd configuration (six wheeled) with respect to the 2nd configuration (4 wheeled) implies possible negative coefficient in the next configuration (8 wheeled). The maximum level of distance at which an object can be pushed was also obtained. This was called the state of plateau wherein adding another module is no longer suggested as it will not improve the pushing capacity any further. Knowing these key points significantly helps in ensuring cost and work efficiency of a given configuration in performing different missions.**

***Keywords*—carrying capacity, cooperative pushing, modular mobile robot, pushing kinematics, single contact point, symbiosis**

I. Introduction

The interaction of robots with the objects surrounding it comes in various forms and presents diverse corresponding challenges. There are so-called established paradigms representing a robotic movement and "pushing" is one of these compelling primitives that can expand the robotic interaction and manipulation of objects [1]. In rescue operations for instance, lifting debris from a collapsed building to create a passageway to trapped victims is a labor-intensive mission to perform for industrial robots [2]. Pushing these debris is more practical and easier to accomplish than lifting it. In the manufacturing industry, mobility of heavy materials in warehouses by means of dragging is an everyday industrial robotic manipulation task [3]. For the most part though, pushing objects is not as easy as it sounds especially to materials that require immense safety handling. Pushing objects demands careful assessment of various external forces to avoid erratic moving direction leading to catastrophic outcomes [4]. Making efficient use of multi-cooperative mobile robots extends the pushing capacity of a single mobile robot. To achieve this, several constraints in the manipulation point of view such as but not limited to information sharing and intelligent coordination, need to be worked on [5]. Research studies on predicting the movements of both the pushing multi-cooperative mobile robot and the object being pushed are particularly associated with the scholarly works of Lynch [6], which claims that determining the motion of an object being pushed can be attained more accurately with more contact points, and Erdmann [7], which analyzes the orientation and motion of an object based on the perceived contact point of the pushing fingertip. The solid theoretical foundation on this segment paved the way to several simulated environment applications. The change in velocity of a modular robot was examined when performing certain missions in different configuration types using MATLAB simulink [8]. Using the same software application, a micro maqueen robot was modeled

Manuscript received July 31, 2023; revised September 13, 2023; accepted November 24, 2023; published April 29, 2024.

in another study. Its ability to replicate the performance of the actual robot was counterchecked for suitability in future experiments [9]. The pushing navigation of a humanoid robot was observed in a common indoor environment to simulate its performance on alleys in the works of Scholz *et al.* [10]. Despite the existence of these research studies, there is still a need to advance these to meet the standards of more intricate pushing operations. Experts of the field figured out that the root cause of slow-moving progress and disconnection in robotic studies is the insufficient evaluation metrics and corresponding benchmark. Heavy computing algorithms such as computer vision are anchored with quantitative metrics. The planar pushing capacity was improved through the control of direction, distance, and speed [11], neural network and regression models were used as a method for optimization [12], and heavy training, testing, and validation datasets [13] were used in various studies. Hence, a clearer direction on research development although studies of this kind commensurate with a vast dataset which is a soft spot of robotics [14]. The fundamentals of pushing operations performed in the cited works are explained in the theoretical considerations in the next section. Similarly, the specific models used in the heavy computing algorithms mentioned above are elaborated.

This study aims to address the gap in benchmarking specifically to multi-cooperative robots by providing a baseline methodology for analyzing configurations of practically any type. In this method, the symbiotic level of a configuration will be measured such that a performance can still be assessed in the absence of reference benchmark values, consequently, opportunities for improvement can be both identified and quantified. Pushing operation was focused on the implementation of the study and the method referred to is symbiosis, a biosystem-inspired approach on describing interactions. The application of symbiotic phenomenon to the performance analysis of a multi-cooperative mobile robot serves as the novelty of the study. The motivation of the study is to follow through the preceding study of the researchers on linear traversal mission of the designed multi-cooperative robots. In the next phase, the researchers aim to cover more missions such as climbing and crossing gaps to obtain the most conducive symbiotic coefficient given a configuration of a multi-cooperative robot.

The structure of the paper next to this section consists of the related work, methodology, results discussion, conclusion, and references. The background and related work section presents supporting theories for the applied method and existing approaches for the identified problem domain. The materials and method section showcases the parameters, robotic design, and the analysis method or algorithm applied. The corresponding output of the experiments conducted was explained in the results and discussion section. Finally, the achievement of the objective including the rooms for improvement are stated in the conclusion and future works section.

II. Background and Related Work

This section discusses the theoretical and design considerations of the study and is divided into two, namely load model and symbiotic approach.

A. Load and Pushing Interaction Model

In non-prehensile robotic manipulation such as pushing, finding the most stable configuration requires rigorous understanding of forces acting on the body of the robot and the object it interacts with [15]. At the very least, two conditions must be maintained: (1) wheels of a mobile robot contact with the ground [16], and (2) contact between the horizontal planar centroid of the wheeled robot and the object being pushed [17]. The Taguchi method was used in a study [18] to optimize the 1st condition. In this method, it analyzes the kinematic constraints of a robot through multiple trials of climbing a platform until the best parameter values were drawn out to reach the highest level without losing contact to the ground and falling. In Fig. 1, the parameters that were considered in different configurations and series of trials are labeled in the schematic diagram of the wheeled robot. The analysis of height constraints for the first and last two wheels to be able to climb up together were illustrated in Fig. 1(a) and Fig. 1(b) respectively.

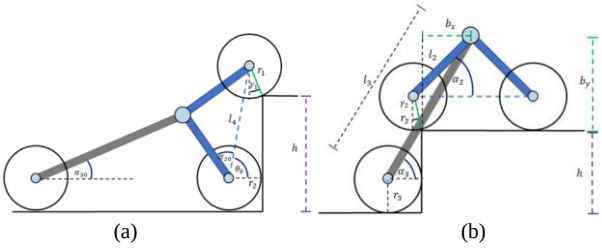

(a) (b)

Fig. 1. Wheeled robot kinematic constraints on climbing for (a) front and middle wheels and (b) middle and back wheels [18].

Taguchi method was utilized as a quality control approach to augment the proposed symbiotic assessment method in this study. The results per iteration per experiment run within the permissible limit of factors or constraints will be discussed in detail in Section IV of this paper.

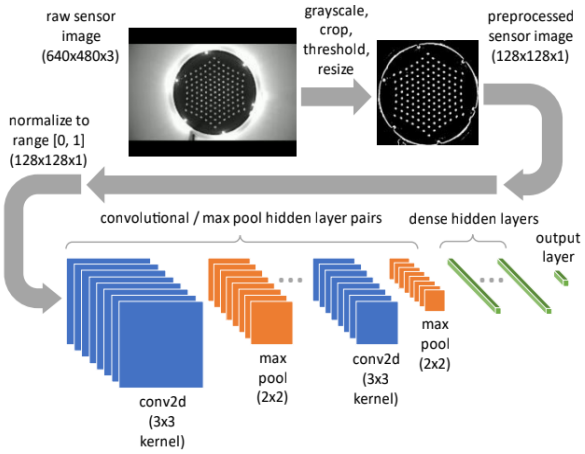

Fig. 2. Sensor pose prediction using Convolutional Neural Network (CNN) model [15].

In another study, tactile sensing and proprioceptive feedback mechanism were used to attain the 2nd condition on maintaining stable contact between the robot and the object being pushed [15]. Universal Robotic Arm UR5 was attached with a TacTip sensor and configured to work with a CNN model forming their so-called tactic servoing control subsystem. CNN analyzes the image acquired through the optical sensor to determine the arm's positioning relevant to a box (object being pushed) as illustrated in Fig. 2. It is a closed loop process that allows continuous calibration of the arm's position to ensure that during the pushing operation, its distance and angular orientation are fixed relative to the box.

Another control subsystem establishes the pushing direction of the arm towards the target destination. This time, the arm's central axis orientation relative to the target is being manipulated through its perceived center of friction (CoF). It does so by achieving a zero error $\varepsilon = \theta' - \theta$ value of bearings, where θ' is the observed and θ is the reference target, and adding another corrective variable ${}^{s''}u_{s'''}$ to the tactic servoing corrective factor ${}^{s}u_{s'''}$. Both of these corrective factors were calculated according to the PID control law [15]. Refer to Fig. 3 for better visualization of this.

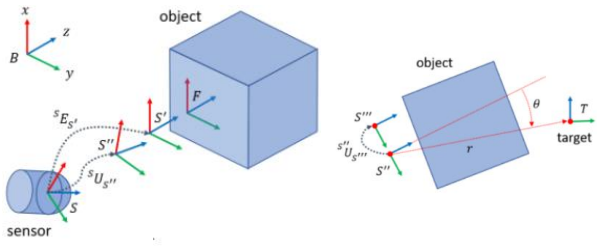

(a) (b)

Fig. 3. Calculation of target bearing using the two control subsystems' corrective factors considering (a) pusher position and (b) target bearing [15].

The same planar considerations using the same cubic object were adapted in this study. However, instead of using a heavy computing model for recalibration, a light-weight approach is proposed in this study. Besides, using the CNN model leads back to the research gap identified in terms of benchmarking given a lot of metrics to evaluate as well. In this study, physical configuration was focused on to bring out the so-called calibration or corrective factor instead of heavy computational algorithms, consuming much power and requiring expensive electronics subcomponents for a robot [19].

More of the planar pushing interactions were presented in the study of Yu [14] comprising about a million high-fidelity datasets experimented in various dimensions such as the shape of the object being pushed, the material of the surface, the speed and acceleration of pushing activity, the contact position, and the angular direction. The insights on shape with varying load, surface, and direction were of particular use in this study. A hollow cubic object with concentrated load allows simulation of solid objects with presumably, equal pressure distribution along the *x*-axis [14]. This phenomenon contributes to lesser variation of frictional force which is highly preferred in experimental setups as in this study. The surface material on the other hand, dictates the degree at which an object slides. This is influenced by several variability as presented in Fig. 4. Spatial-based variation as in Fig. 4(a) shows that wood surface and polyurethane have higher distribution of friction coefficient depicted with a darker shade. The temporal variability is the only downside for wooden surfaces because of its longer break-in period as shown in the trend in Fig. 4(b). In terms of speed and direction, there is higher consistency for wood material as shown in Fig. 4(c) and Fig. 4(d). To conclude, wooden material was chosen for this study given its acceptable variability and availability.

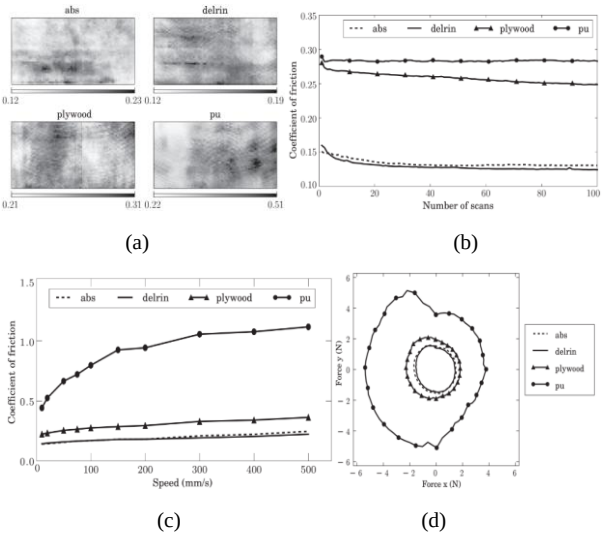

(a) (b)

(c) (d)

Fig. 4. Surface dynamic friction variability based on (a) spatial, (b) temporal, (c) speed, (d) direction.

For pushing direction, the study focused on the 90-degree angle or simply along the vertical axis. Any introduction of trajectory or deviation along the y-axis of the object being pushed, during the pushing motion, was still considered given that the 5 s duration was completed without falling off the platform.

An extension of Yu's study was conducted with the addition of over a hundred more objects under Omnipush dataset, more of the controlled environment for quasi-static pushing interactions rather than variations on dimensions, and prediction models more than actual experimentation [1]. Prediction model was developed as well in another study with the motivation of making its robot adaptive to the dynamicity of the surroundings [20]. The same motivation for working with cluttered environments holds true to the study of Krivic and Piater [21] but making use of the modular approach on the robotic design rather than the prediction model. Multi-cooperative robots used in this study considered this modular approach in conjunction with a bio-system inspired model on evaluating pushing interaction in a semi-controlled environment. The study also considered the insights from the results of Behrens [17] regarding the behavior of a sliding object relative to the direction of the pushing robot and its point of contact. The pushing operation was set at a constant velocity and predetermined values for distance traversed. Fig. 5 illustrates the

experimental setup in a coordinate system model to numerically describe how it works.

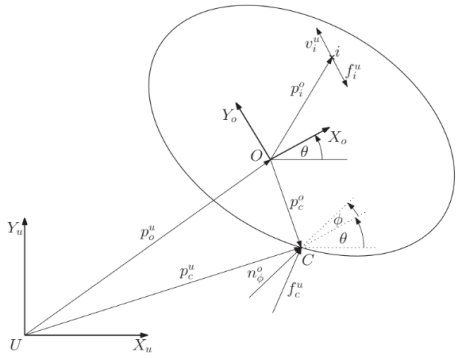

Fig. 5. Object O motion relative to the single contact point C [22].

The study is mainly concerned with the parameter θ which signifies presence of displacement from the original direction of the object being pushed. It is important to keep its value at zero because at a certain point of rotation, the wheeled robot may lose contact from the object being pushed. These instances were not discounted from the evaluated results, although data derived from these are considerable as noise or an outlier at the worst. According to Behren's analysis, this parameter is directly proportional to the pushing speed v_c and can be computed as a function of the pushing angle φ as in Eq. (1). Hence, skewing must not be introduced on the pushing robot. This can be prevented through careful observation on the surface material since it determines the consistency of the frictional force f^u_i acting on the wheels directly affecting the pushing force f^u_c as can be proven in Eq. (4). Derivations of other variables can be referred to Behren's study [17].

$$\theta' = v_c\psi(\varphi) \quad (1)$$

The object's movement is further described numerically in Eqs. (2) and (3).

$$\dot{x} = v_c cos(\theta + \varphi) + v_c\psi(\varphi)(x^o_c sin\theta + y^o_c cos\theta) \quad (2)$$

$$\dot{y} = v_c sin(\theta + \varphi) + v_c\psi(\varphi)(x^o_c cos\theta + y^o_c sin\theta) \quad (3)$$

$$f^u_c = mp^u_o' - \sum_{i=1}^{n} f^u_i \quad (4)$$

A summary of notations used in the analysis of robotic motion is shown in Table I. This includes the description and measurement unit expected on variables used in the equations presented.

In summary, various pushing interactions correspond to different design and kinematic considerations. Approaches from existing related studies were discussed. It can be inferred that while the methodologies presented do address the common constraints in robotic pushing to achieve quasi-static state, cohesiveness and continuity are the lacking attributes. As a result, the gap on benchmarking, specifically to push manipulation of multi-cooperative robots, still has not been established. The insights discussed, however, are a substantial knowledge foundation for the study.

TABLE I. NOTATIONS USED IN ROBOTIC MOTION ANALYSIS

Symbol	Description	Unit
θ′	steady state angular velocity	rad/s
vc	pushing velocity	m/s
ψ(φ)	function of pushing angle with respect to distance	rad/m
θ	rotation angle	rad
φ	pushing angle	rad
xoc	horizontal displacement component	m
yoc	vertical displacement component	m
$\dot{x}$	resulting velocity along *x*-axis	m/s
$\dot{y}$	resulting velocity along *y*-axis	m/s
fuc	pushing force vector	N
fui	frictional force vector	N
puo'	acceleration of the center of the mass	m/s^2
m	mass of object being pushed	kg

B. Multi-Cooperative Mobile Robots

The exploration capabilities of unmanned ground vehicles were improved to great extent with the implementation of the so-called multi-agent systems [23], especially to homogeneous robots. Modular robots with similar build, working together, allow overcoming missions that cannot be done individually such as climbing at certain slope, travelling at certain speed, and pushing at certain distance [8]. Cooperative task performance can be classified as either centralized or decentralized [24]. Centralized mechanism is like a server-client configuration wherein a single robot controls the movement of connected robots. On the other hand, decentralized setup is like peer-to-peer connection wherein cooperating robots individually contribute to the movement of the connected robots acting as a single system [24]. This study applies to the latter. Despite the dynamicity and reconfigurability of decentralized systems, these pose integration issues affecting its morphology [25]. Let's say, a single modular robot can travel a 1 m distance in 10 s. Connecting to another modular robot doesn't guarantee a doubled distance travelled within 10 seconds. Similarly, a single module which can climb 2 steps of a ladder cannot necessarily climb 4 steps of a ladder when added with one more module. Factors such as weight and power consumption of additional modules may affect the performance of existing modules and of the whole system. It can either improve or compromise the operating conditions of one another [23]. In cooperative pushing for instance, additional module certainly contributes more force to the front module in contact with the object being pushed. However, it may run out of power faster and result in a sudden tip-over or rotation of the robotic system [4]. Many other unwanted phenomena may happen if this issue in synergy is not taken seriously [4]. As a resolution, this study implemented a morphological approach to analyze whether a specific configuration can carry out a cooperative mission well or not and to what extent. The method of analysis is further discussed in the next section.

C. Symbiotic Phenomenon

Defining relationships formed between entities whether in biological, social, or economic perspectives, can be attained through a so-called symbiosis. This phenomenon originated from the interaction between organisms which can be classified as mutual, commensal, or parasitic [26]. Mutual relation happens when the interacting organisms benefit from each other. The waste of a clownfish which is rich in ammonia serves as a fertilizer to sea anemone. The latter serves as a shelter and protection to the territorial fish with the help of its stinging tentacles. Influencers promote products in return for sponsorship. Government agencies fund institutions to enable research projects that will bring out development to the society. When only one party benefits, it forms either a commensal or parasitic relationship. The difference between the two is that the latter harms the other. Chameleons benefit from trees when it camouflages to protect itself from predators and also to attack its prey. The trees do not necessarily benefit from chameleons but do not get harmed as well so this can be described as a commensal interaction. The same applies to soldiers taking advantage of nature to disguise itself from their enemies during a war. Greenhouse gas emitted from vehicles causes significant change in climate temperature which ultimately disrupts the weather condition patterns. People benefit in general from the natural resources but harms the environment in return and the use of vehicles on the road is only one of these detrimental instances. This portrays parasitic interaction. These relationship principles in symbiosis were used in the study to predict the effect of various configurations of the mobile robot model in terms of its pushing capacity. The degree of symbiotic relationship a configuration is at, was measured as the quantified value for classifying interaction results.

In a study on multiagent systems, the concept of symbiosis was applied to construct a framework that will represent the emerging behavior from complicated relationships of multiple people or organizations forming a partnership [27]. The result is represented as a symbiotic vector in a two-dimensional plane where the basis of performance is the profit obtained from company 1 on x-axis and company 2 on y-axis. The same concept was applied to a trash collection in a community where the interacting entities were robotic trash collectors. Based on the work efficiency measured through the amount of trash collected and electric charge consumed, the symbiotic relationship was defined [28]. In addition to the robotics domain, symbiotic adaptive multi-simulation was used to control an unmanned aerial vehicle [29] and to plan the optimal path for an unmanned ground vehicle under various environmental conditions.

The symbiotic phenomenon applies to several domains outside biosystems. Applied researches adopted its concept to processes including decision making, control, optimization, and validation. Although, several research issues are still open as cited in the study of Aydt *et al.* [30]. The involvement of actual physical systems is suggested to overcome these. In this study, actual mobile robots were designed to perform pushing tasks in a multi-cooperative manner.

Herein, these modular robots serve as agents or entities interacting with one another. Its emerging behavior was assessed based on the pushing capacity result per configuration state under various loads. With this study, the baseline assessment for multi-cooperative mobile robots was made possible in response to the identified gap in robotics, which is primarily benchmarking. The use of symbiotic approach in the study helps draw out the coefficient permission or operation such as pushing. With these coefficients, the optimal configuration can be determined progressively and in a more sustainable way. Meanwhile, benchmarking is required in the existing studies to determine optimal performances of robots. This entails heavy consumption of time and resources.

III. Materials and Methods

Pushing is typically the basic skill and task of a robot. The mission of the robot is to deliver or move the object from one point to another. In some cases, however, the task cannot be completed. Also, the load is beyond the pushing capacity of the robot. For this reason, the researchers of the study propose to analyze the capability of a single robot in pushing and to study the effect of cooperative pushing through a single contact point of pushing. According to Stüber *et al.* [1], various approaches in making analysis can be classified into purely analytical, hybrid, dynamic, physics engine-based, data driven, and deep learning-based. Purely analytical is the basic foundation and mechanics. It requires understanding of the external and internal forces involved in the pushing task and of the movement of the two bodies in contact which are the pusher and the object being pushed. The challenge here is predicting the motion of the object being pushed in relation to the contact surface and the frictional force. However, this approach has limitations as it tends to become more complex, especially when taking the real-world factors into consideration.

Purely analytical examination best suits the ideal world scenario as compared to actual applications [15]. Data driven approach is an estimate-based observation that is much realistic yet prone to uncertainties due to the different parameters to consider on the side of both the pusher and the object being pushed. On the other hand, Physics engine and dynamic analysis offer great value for application through dynamic interaction and 3D objects.

However, these approaches require explicit object modeling and extensive parameter tuning, prediction, and motion from data [31]. Deep learning is a method that employs artificial intelligence algorithms to learn extensively from vast and sparse data [12].

A. Parameters

A two-wheeled mobile robot was used to push a hollow cube with a dimension of 10×10 cm. Calibration weights, as shown in Fig. 6, were used to vary the load on the hollow cube. As discussed in the previous section, cubic shape allows approximately equal distribution of pressure with respect to the horizontal axis. In addition, certain

materials affect the degree to which an object slides during a pushing activity. It is to be noted that the material used for objects in contact is Polylactic Acid (PLA). This is typically what 3D printed objects are made of.

(a) (b)

Fig. 6. Experiment components (a) calibration weights (b) carrying object.

The platform, on the contrary, is a laminated wood. The rationale is its acceptable variability as mentioned as well in the previous section and its accessibility in general. The experimental setup and corresponding equations for the computational model used in single and cooperative pushing manipulations will be discussed in the next subsections.

The initial experiment was performed in a simulated environment using MATLAB Simulink (see Fig. 7(a)). A primitive box load was created with a plane contact force to the floor. Then, pushing activity was performed but it didn't work out. The robot only passes through the primitive created. There is no change in distance traversed and the big body doesn't affect the primitives. Density and friction factors were tried to be changed as well but to no avail. The individual capability of a mobile robot in a single pushing task was tested to check how much load it can push in an actual design experiment instead (see Fig .7(b)). A DFRobot Micro Maqueen Lite was used as the internal electronic component for each of the modular mobile robots. The DFRobot runs on a 32-bit ARM Cortex M0 CPU. It has an approximate dimension of 81 mm × 85 mm × 44 mm and has an estimated mass of around 76 g. The motor can rotate up to a speed of 133 rpm.

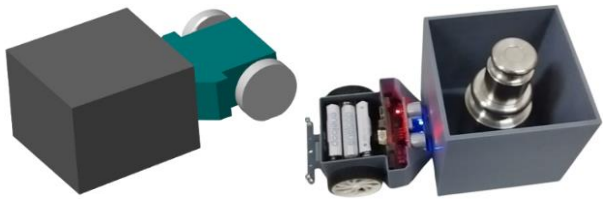

(a) (b)

Fig. 7. Single pushing through (a) Matlab Simulink simulation and (b) actual design experiment.

The ranges of experimental values used in this study are summarized in Table II. The first thing to do is to identify the carrying capacity (in terms of pushing) of an individual module/species thru actual experimentation on different sets of loads then later testing it on different no. of module configuration. Fig. 8 shows the process in identifying the pushing carrying capacity in the experimental methodology.

TABLE II. RANGES OF EXPERIMENTAL INPUT PARAMETERS

Input Parameters	Range
No. of Modules	1, 2, 3, N_1, N_2, N_3
Load	1–2 kg

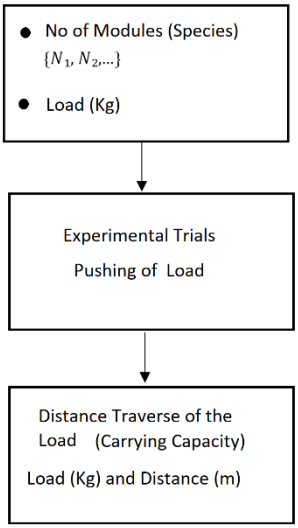

Fig. 8. Experiment process diagram.

B. Experimental Set-up

The researchers chose the data driven approach in terms of actual experimentation with the initial assumption using the basic mechanics of analytical approach.

1) Single pushing

Investigating the motion of the object sliding in the surface can be better understood by first identifying the forces acting on the bodies through the free body diagram illustrated in Fig. 9. Here, it can be seen that a single pushing activity entails vertical force in the form of mass influenced by gravity, and horizontal forces in the form of frictional forces through the object and mobile robot wheel opposing the applied pushing force produced through the wheel torque.

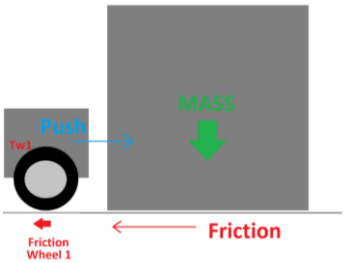

Fig. 9. Free body diagram of single mobile robot.

Through Eqs. (2) and (3) the new position coordinates of the object in a plane, after single pushing, can be determined. Using the distance formula as in Eq. (5), the distance traversed D_t can be calculated where x and y are the coordinates of the object's original position and x' and y' are the coordinates of the object's new position when pushed.

$$D_t = \sqrt{(x^{\cdot} - x)^2 + (y^{\cdot} - y)^2} \quad (5)$$

Alternatively, distance can be calculated by getting the difference of the object's new absolute position p^u_o' and origin position p^u_o. Recall that these positions are driven by both the frictional forces (wheel to ground and load to ground contact forces) and pushing forces (driven by wheel torque T_w) as in Eq. (4). The absolute position is given by Eq. (6) where p^u_c is the position of the contact point of the robot body to the object being pushed relative to the ground, p^o_c is the position of the contact point relative to the object, and R^u_o is the rotation matrix as in Eq. (7).

$$p^u_o{}' = p^u_c - R^u_o p^o_c \quad (6)$$

$$R^u_o = [^{cos\theta}_{sin\theta} \; ^{-sin\theta}_{cos\theta}] \quad (7)$$

These equations are under the assumption that pushing activity is performed at a constant velocity with the robot having a single contact point to the load. The same applies with the addition of mobile robots performing the task in a cooperative manner. The analysis this time, however will be applied with the symbiotic approach and corresponding equations to be discussed in the next subsection.

2) Cooperative pushing

In this paper, the researchers are proposing if the symbiosis model is indeed applicable in a linear pushing task in which the individual homogenous modules are cooperating in moving or pushing the load in front of it as in Fig. 10. Several mathematical models were presented in the study of Yukalov on symbiosis applied in the livelihood of coexisting agents [27]. These models cover general, mutual, asymmetric, and indirect interactions. The general model was considered in the study as this encompasses the derived equations which serve as the fundamentals of symbiosis.

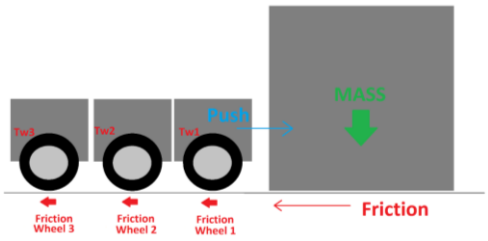

(a)

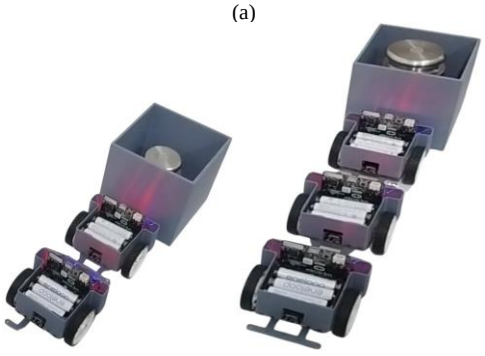

(b) (c)

Fig. 10. Cooperative pushing: (a) free body diagram (b) actual four wheeled and (c) six wheeled robot.

C. Data Analysis

To derive the carrying capacity function in cooperative pushing, the mathematical model in Eq. (8) was used. This also determines the relationship class or the connection of multi-wheeled robots to each other whether harmful, beneficial, or neutral through the symbiotic coefficient β. M refers to the total carrying capacity of a specific configuration, i for number of modular mobile robots in a given configuration, α for single pushing capacity, and $S_i(\{N_1\})$ for the function describing the influence of interacting modules to one another. This function varies from one domain to another. In this study, the domain is a multi-agent system where the carrying capacity being measured is the distance and the interaction function is the function of the distance with respect to the number of cooperative robot pushing. The working kinematic equations are as discussed in the previous sections.

$$M = \alpha_i + \beta_i \, S_i(\{N_1, N_2, \ldots\}) \quad (8)$$

The conditional values from Eqs. (10) to (12) classify the assessment per configuration at various loads applied. Negative symbiotic coefficient corresponds to an undesirable configuration, positive to a desirable one, and zero to an acceptable configuration. The single pushing capacity α must be a non-zero value and the symbiotic coefficient can be any integer in the number system as in Eq. (9).

$$\alpha > 0, \quad \beta \in [-\infty, \infty] \quad (9)$$

$$M > \alpha, \quad \beta \in (0, \infty] \quad (10)$$

$$M = \alpha, \quad \beta = 0 \quad (11)$$

$$M < \alpha, \quad \beta \in [-\infty, 0) \quad (12)$$

A list of symbols used in equations for the methodology section is shown in Table III for easier reference of variables and corresponding measurement units.

TABLE III. NOTATIONS USED IN METHODOLOGY SECTION

Symbol	Description	Unit
θ'	steady state angular velocity	rad/s
Dt	relative displacement after pushing	cm
$x^{\cdot}$	final horizontal displacement	cm
x	initial horizontal displacement	cm
$y^{\cdot}$	final vertical displacement	cm
y	initial vertical displacement	cm
puo	new absolute position	cm
puc	position of the contact point relative to the ground	cm
Ruo	rotation matrix	rad
poc	position of the contact point	cm
θ	rotation angle	rad
M	total carrying capacity	cm
α	single carrying capacity	cm
β	symbiotic coefficient	unitless
$S(\{N\})$	function of distance with respect to no. of cooperative robot pushing	cm

The experiment trials conducted for study are summarized in Table IV. This includes the number of experiments performed, the number of trials for each experiment, the mode, the number of interacting robots tested per trial, and the load applied per trial.

TABLE IV. EXPERIMENT TRIALS

Experiment Number	Mode	Total Number of Trials	Number of Modular Mobile Robot	Weights (in kg)
1	Simulation	1	1	-
2	Actual	23	1,2,3	1, 1.4, 1.5, 2, 3
3	Actual	30	1,2,3	1, 2
4	Actual	90	1,2,3	1, 1.2, 1.5, 1.7, 2

It can be noticed that the number of experiments in simulation mode as well as the trial and number of modules is only one because doing the pushing mission using Simulink did not materialize due to software constraints. The experiments and trials per experiment in actual mode were implemented in increasing value. This is because the researchers need to initially find the perceived optimal controlled environment to ensure a more reliable experimental results as Taguchi method suggests (discussed in Section II). In terms of the load, the weights were also gradually increased for each trial. The 4th experiment needs to be performed to supplement the 3rd experiment. This helped the researchers see the granular trend of the resulting carrying capacity for each configuration. Fig. 11 shows the process on how the researchers draw out the symbiotic coefficient and identify the effect if it is harmful, beneficial or no effect in a given configuration. The insights from the experiment results were discussed in the next section.

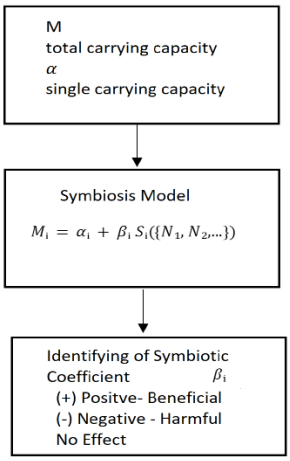

Fig. 11. Data analysis process diagram.

IV. RESULTS AND DISCUSSION

Actual tests were carried out with two varying loads (1 kg and 2 kg) and three different configurations (2 wheeled, 4 wheeled, and 6 wheeled configurations). Distance was measured and compared across different loads and configurations analyzing if there is an effect on the overall carrying capacity in a group configuration.

Based on the pushing experiment results (refer to Fig. 12), it has been tested that one module can move a 1 kg calibration weight at an average distance of 0.6 m within 5 s. Having the same load at 1 kg but this time with a two or three module configuration, yielded to almost similar displacement recorded at 0.75 m. When a 2 kg load was used, one module can no longer push the object. However, with two modules connected together, the distance traveled was 0.24 kg. A three modules configuration doubled the distance traveled pushing the same load.

The distance traveled in a pushing mission depends on the amount of load and other factors such as frictional force, and module torque capacity. It can be hypothesized in this setup that, at a certain minimum load no matter how many modules were pushing, the distance will still remain the same provided that the same parameters were maintained such as the velocity/speed, torque, friction, pushing orientation and surface material.

The second iteration was performed with varying loads of 1, 1.2, 1.5, 1.7, and 2 kg. The purpose of this iteration is to check the distance response curve on changing loads.

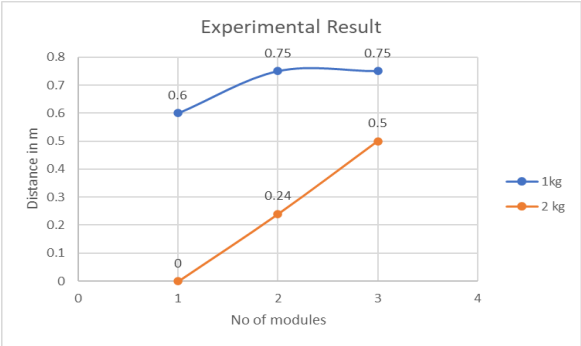

Fig. 12. Carrying capacity trend in pushing mission under two varying loads.

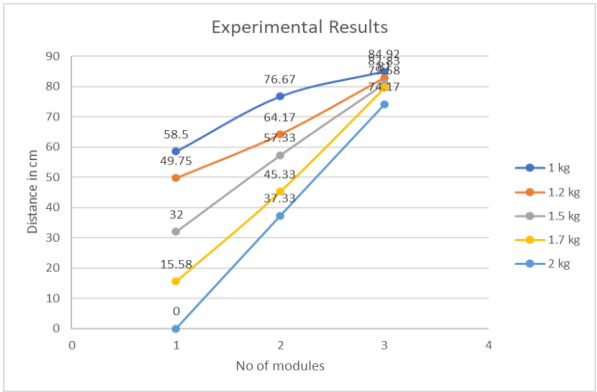

Fig. 13. Carrying capacity trend in pushing mission under 5 varying loads.

The graph in Fig. 13 shows that the heavier the load applied, the pushing capacity effect in terms of distance traversed is evident with the increasing number of modules connected in a configuration as well. In the first iteration, recall that single pushing can move a 1 kg box load to a 0.60 m distance. But as the load to push increases, the distance traveled decreases up to a point (so-called stagnation point) where the object can no longer be pushed

any further. Despite increasing the number of modules, the trend reaches a state of plateau relative to the pushing distance.

The actual distance traversed per trial in the second iteration is illustrated in Fig. 14. Here, it can be deciphered much more clearly that the pushing capacity limitation of any of the three configurations is within 0.7 to 0.8 m distance. The vertical component differences in pushing capacity at various loads were more visible on lower configurations but as it goes any higher as in the 6 wheeled configuration, it can be seen that the pushing capacity falls within 0.2 unit vertical distance range. This narrower vertical difference at higher configuration effectively supports the plateau condition as observed in Fig. 13.

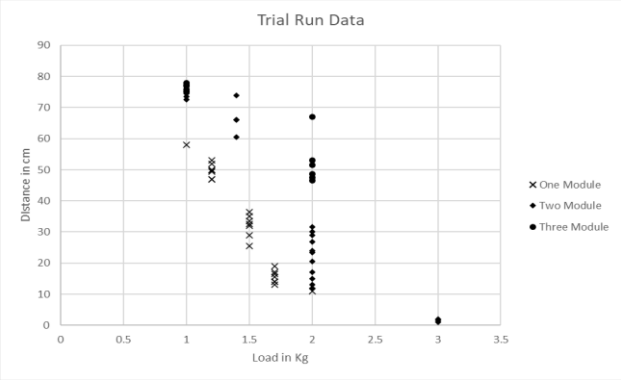

Fig. 14. Second iteration distance results per configuration u nder 5 varying loads.

Applying the symbiosis approach, Tables V and VI summarizes the corresponding derived symbiotic coefficient for the 1st and 2nd iteration. Recall that in cooperative pushing, the symbiotic coefficient in the 2nd term of the linear equation Eq. (5.1) determines the symbiotic relationship classification of a given configuration. The table consists of 4 main columns showing the values for the load, the single pushing capacity, the symbiotic coefficients of 2 and 3 module configuration with respect to the initial carrying capacity, and finally, the symbiotic coefficients of 2 and 3 module configuration with respect to the carrying capacity of the preceding configuration.

It can be seen that all symbiotic coefficients (except for one) resulted with a positive sign implying mutual or beneficial influence of interacting modules to each other while performing the pushing mission under various loads and configurations. Essentially, the designed configurations of modular mobile robots were suitable for the pushing operation in general. Although, there are some key observations from the tabulated values. One is that the symbiotic coefficient (numerical value in red color) for 3 module configuration pushing 1 kg load in the 1st iteration is 0. This signifies neutral interaction which means there is no benefit nor harm effect when another module was added to the 4 wheeled mobile robot doing the cooperative pushing. Hence, the 3rd configuration may or may not be considered for pushing a 1 kg load since the addition of one more module did not add up anyway to the overall cooperative pushing capacity. Another point of observation are the numerical values in orange color. While it is clear that the positive sign signifies beneficial influence, it is worth considering that the numeric value is lower as compared to the preceding configuration. This means that the 3rd configuration in various loads may still be beneficial in terms of overall carrying capacity, but the diminishing value leads to an insight that going for the next configuration may not be worthwhile.

TABLE V. SYMBIOTIC FUNCTION VALUES FOR 1ST ITERATION

		wrt to initial carrying capacity		wrt to previous carrying capacity	
Load	α	β_2	β_3	β_2	β_3
1 kg	60	(+) 0.2500	(+) 0.2500	(+) 0.2500	0.0000
2 kg	0	(+) 1.0000	(+) 2.0833	(+) 1.0000	(+) 2.0833

TABLE VI. SYMBIOTIC FUNCTION VALUES FOR 2ND ITERATION

		wrt to initial carrying capacity		wrt to previous carrying capacity	
Load	α	β_2	β_3	β_2	β_3
1 kg	58.5	(+) 0.3106	(+) 0.4516	(+) 0.3106	(+) 0.1076
1.2 kg	49.75	(+) 0.2898	(+) 0.6649	(+) 0.2898	(+) 0.2908
1.5 kg	32	(+) 0.7916	(+) 1.5313	(+) 0.7916	(+) 0.4129
1.7 kg	15.58	(+) 1.9095	(+) 4.1078	(+) 1.9095	(+) 0.7556
2 kg	0	(+) 1.0000	(+) 1.9869	(+) 1.0000	(+) 0.9869

To check the validity of the model established thru experimental data a regression analysis was use to check the influence of the load and number of pushing modules to the outcome of the distance move traverse by the load. Upon executing the analysis, it shows the load and modules change by a unit, associated with the coefficient indicates the changes. As seen in Table VII the correlation of the variables has a 95% level of confidence. The variance has an output of 0.92 and the adjusted R square has a value of 0.91 which overestimate the coefficient of the variables. The Anova in Table VIII shows the context that significance value is 6.78 E-7 and is smaller than 0.05 and thus we reject the null hypothesis that the coefficients are 0 and say that the data is reliable and is below the threshold. The p-values in Table IX are all less than 0.05 threshold means that greatly influence the output variable.

TABLE VII. REGRESSION STATISTICS

Regression Statistics	Value
Multiple R	0.96
R^2	0.92
Adjusted R^2	0.91
Standard Error	8

TABLE VIII. ANALYSIS OF VARIANCE

df	SS	MS	F	Significance F
2	8698.43	4349.21	67.27	6.78E−07

TABLE IX. SIGNIFICANCE OF REGRESSION MODEL

Sources of Variation	Coefficients	Standard Error	*t*-Stat	*p*-value
Intercept	51.51	11.96	4.31	0.0012
Load	−32.82	6.34	−5.18	0.00031
Module	26.04	2.72	9.5	1.12E-06

V. Conclusion and Future Works

This study presents a baseline methodology to assess the suitability of different configurations in doing a cooperative pushing of varying loads. Leveraging the symbiosis phenomenon, the influence of additional modules to existing modules in terms of the carrying capacity (pushing in this case) was analyzed. Experiments were tried out both in simulation and actual mode.

The results were analyzed through a data driven approach with the consideration of the load and pushing interaction kinematics. Based on the results of the iterations carried out, it can be concluded that (1) symbiotic coefficient indeed provides immediate valuation of configuration whether it will be beneficial, neutral or harmful to the whole system, (2) cooperative pushing reaches stagnation point at heavier loads irregardless of adding more modules, and (3) 6-wheeled mobile robot is the optimum configuration to perform cooperative pushing up to 2 kg load. With these key insights, it is recommended to (1) explore less constrained experiment setup, (2) apply the proposed method to other common missions of mobile robots such as pulling, climbing, and carrying, and (3) do regression on coefficient results to extend the use case of the study from assessment to prediction analysis.

Dataset acquisition is a soft spot in robotics leading to benchmarking gaps in the existing studies [14]. Assessment of the design configurations is crucial on cooperative modular mobile robots [26]. Assessment cannot be performed without reference or benchmark values. With the proposed symbiotic approach, evaluating configurations can now be implemented through the resulting symbiotic coefficients. This is the core contribution of the study, especially in the field of modular mobile robotics.

Conflict of Interest

The authors declare no conflict of interest.

Author Contributions

A. Fernando conducted the research and wrote the paper; M. Guillermo helped draft the paper; L. Gan Lim mentored the researcher; A. Bandala, R. R. Vicerra, E. Dadios, and R. Naguib assisted in research consultation; all authors had approved the final version.

Acknowledgment

The authors wish to thank their respective institutions for the assistance in conducting and completing this research study. The authors also acknowledge the funding support from the Department of Science and Technology (DOST) Philippines through its Engineering Research and Development for Technology (ERDT) academic scholarship program.

References

[1] J. Stüber, C. Zito, and R. Stolkin, "Let's push things forward: A survey on robot pushing," *Frontiers in Robotics and AI*, vol. 7, 2020.

[2] J. S. Yang, S. Ogawa, T. Tsujita, S. Komizunai, and A. Konno, "Massive object transportation by a humanoid robot," *IFAC-PapersOnLine*, vol. 51, no. 22, pp. 250–255, 2018.

[3] J. Lee, J. Lee, J. Kang, S. Park, and D. Jang, "Prediction of robot technology using multi-phase model," *Journal of Advances in Information Technology*, vol. 11, no. 3, pp. 181–185, 2020.

[4] B. Ghotbi, F. González, J. Kövecses, and J. Angeles, "Effect of normal force dispersion on the mobility of wheeled robots operating on soft soil," in *Proc. IEEE International Conference on Robotics and Automation (ICRA)*, Hong Kong, China, 2014, pp. 6612–6617.

[5] M. Murooka, S. Nozawa, Y. Kakiuchi, K. Okada, and M. Inaba, "Whole-body pushing manipulation with contact posture planning of large and heavy object for humanoid robot," in *Proc. IEEE International Conference on Robotics and Automation (ICRA)*, Seattle, WA, USA, 2015, pp. 5682–5689.

[6] K. M. Lynch and M. T. Mason, "Stable pushing: Mechanics, controllability, and planning," *International Journal of Robotics Research*, vol. 15, no. 6, pp. 533–556, 1996.

[7] J. Y. Bin and M. Erdmann, "Pose and motion from contact," *International Journal of Robotics Research*, vol. 18, no. 5, pp. 466–490, 1999.

[8] A. Fernando and L. GanLim. (2020). Velocity analysis of a six-wheel modular mobile robot using MATLAB-Simulink. in RCMEManuE [Online]. Available: https://iopscience.iop.org/article/10.1088/1757-899X/1109/1/012037

[9] A. H. Fernando and L. A. G. Lim, "Model-based simulation of a mini differential drive robot," in *Proc. IEEE 13th International Conference on Humanoid, Nanotechnology, Information Technology, Communication and Control, Environment, and Management (HNICEM)*, Manila, Philippines, 2021, pp. 1–4.

[10] J. Scholz, S. Chitta, B. Marthi, and M. Likhachev, "Cart pushing with a mobile manipulation system: Towards navigation with moveable objects," in *Proc. IEEE International Conference on Robotics and Automation*, 2011.

[11] M. Bauza, F. R. Hogan, and A. Rodriguez, "A data-efficient approach to precise and controlled pushing," arXiv preprint arXiv:1807.09904, 2018.

[12] A. H. Fernando, I. A. V. Marfori, and A. B. Maglaya, "A comparative study between artificial neural network and linear regression for optimizing a hinged blade cross axis turbine," in *Proc. International Conference on Humanoid, Nanotechnology, Information Technology, Communication and Control, Environment and Management (HNICEM)*, Cebu, Philippines, 2015, pp. 1–4.

[13] A. H. Fernando, A. B. Maglaya, and A. T. Ubando, "Optimization of an algae ball mill grinder using artificial neural network," in *Proc. IEEE Region 10 Conference (TENCON)*, Singapore, 2016, pp. 3752–3756.

[14] K. T. Yu, M. Bauza, N. Fazeli, and A. Rodriguez, "More than a million ways to be pushed: A high-fidelity experimental dataset of planar pushing," in *Proc. IEEE/RSJ International Conference on Intelligent Robots and Systems (IROS)*, 2016.

[15] J. Lloyd and N. F. Lepora, "Goal-driven robotic pushing using tactile and proprioceptive feedback," in *Proc. IEEE Transactions on Robotics*, vol. 38, no. 2, April 2022, pp. 1201–1212.

[16] S. Shirafuji, Y. Terada, T. Ito, and J. Ota, "Mechanism allowing large-force application by a mobile robot, and development of ARODA," *Robotics and Autonomous Systems*, vol. 110, pp. 92–101, 2018.

[17] M. J. Behrens, "Robotic manipulation by pushing at a single point with constant velocity: Modeling and Techniques," PhD. thesis, University of Technology, Sydney, 2013.

[18] N. Pico, S. H. Park, J. S. Yi, and H. Moon, "Six-wheel robot design methodology and emergency control to prevent the robot from falling down the stairs," *Applied Sciences (Switzerland)*, vol. 12, no. 9, 2022.

[19] B. H. Lee, I. H. Yu, and J. S. Kong, "Torque analysis and motion realization of reconfigurable modular robot," *International Journal of Control and Automation*, vol. 6, no. 3, 2013.

[20] C. O. Barcelos, L. A. Fagundes-Júnior, D. K. D. Villa, M. Sarcinelli-Filho, A. P. Silvatti, D. C. Gandolfo, and A. S. Brandão, "Robot formation performing a collaborative load transport and delivery task by using lifting electromagnets," *Applied Sciences*, Switzerland, vol. 13, no. 2, 2023.

[21] S. Krivic and J. Piater, "Online adaptation of robot pushing control to object properties," in *Proc. IEEE/RSJ International Conference on Intelligent Robots and Systems (IROS)*, Madrid, Spain, 2018, pp. 4614–4621.
[22] M. Behrens, S. Huang, and G. Dissanayake, "Models for pushing objects with a mobile robot using single point contact," in *Proc. IEEE/RSJ International Conference on Intelligent Robots and Systems*, Taipei, Taiwan, 2010, pp. 2964–2969.
[23] S. H. Turlapati, A. Srivastava, K. M. Krishna, and S. V. Shah, "Detachable modular robot capable of cooperative climbing and multi agent exploration," in *Proc. IEEE International Conference on Robotics and Automation (ICRA)*, Singapore, 2017, pp. 255–260.
[24] L. Furno, M. C. Nielsen, and M. Blanke, "Centralised versus decentralised control reconfiguration for collaborating underwater robots," in *Proc. 9th IFAC Symposium on Fault Detection, Supervision and Safety for Technical Processes*, 2015, pp. 732–739.
[25] A. Ghosh, A. Ghosh, A. Konar, and R. Janarthanan, "Multi-robot cooperative box-pushing problem using multi-objective particle swarm optimization technique," in *Proc. World Congress on Information and Communication Technologies*, Trivandrum, India, 2012, pp. 272–277.
[26] A. Fernando and L. GanLim, "Symbiotic approach in a modular mobile robot," *International Journal of Emerging Trends in Engineering Research*, vol. 9, no. 5, 602, 2021.
[27] V. I. Yukalov, E. P. Yukalova, and D. Sornette, "Modeling symbiosis by interactions through species carrying capacities," *Physica D: Nonlinear Phenomena*, vol. 241, no. 15, pp. 1270–1289, 2012.
[28] S. Mabu, M. Obayashi, and T. Kuremoto, "Reinforcement learning with symbiotic relationships for multiagent environments," *Journal of Robotics, Networking and Artificial Life*, vol. 2, no. 1, 40, 2015.
[29] P. Tokekar, J. V. Hook, D. Mulla, and V. Isler, "Sensor planning for a symbiotic UAV and UGV system for precision agriculture," *IEEE Transactions on Robotics*, vol. 32, no. 6, pp. 1498–1511, Dec 2016.
[30] H. Aydt, S. Turner, W. Cai, and M. Low, "Research issues in symbiotic simulation," in *Proc. the 2009 Winter Simulation Conference*, December 2009, pp. 1213–1222.
[31] T. Yoshikawa and M. Kurisu, "Indentification of the center of friction from pushing an object by a mobile robot," in *Proc. IROS '91: IEEE/RSJ International Workshop on Intelligent Robots and Systems '91*, Osaka, Japan, 1991, pp. 449–454, vol. 2.